Characterization of stroke lesions using a histogram-based data analysis including diffusion- and perfusion-weighted imaging

Alexander Grzesik (1), Johannes Bernarding (1), Jürgen Braun (1), Hans-Christian Koennecke (2), Karl-Jürgen Wolf (3), and Thomas Tolxdorff (1)

Department of Medical Informatics (1), Department of Neurology (2), and
Department of Radiology and Nuclear Medicine (3)
University Hospital Benjamin Franklin,
Free University of Berlin
Hindenburgdamm 30, 12200 Berlin
Email: grzesik@ukbf.fu-berlin.de

Abstract. Diffusion- and perfusion-weighted magnetic resonance imaging (DWI, PWI) allows the early diagnosis of ischemic brain injury. Regions with pathologic apparent diffusion coefficients (ADC) mismatching with pathologic mean transit times (MTT) or relative cerebral blood volume (rCBV) are thought to correlate with tissues that can be saved by appropriate treatment. Ten patients with cerebral ischemia were examined. Combining different information (T2w, DWI, ADC, rCBV, MTT) into multidimensional histograms allowed the segmentation of ischemic and unaffected tissues and overcame problems with strongly fluctuating parameters. Correlating ADC, T2w, and rCBV with clinical symptoms allowed the estimation of age and perfusion state of lesions.

Keywords: Segmentation, MRI, Diffusion, Perfusion, Image Processing

1 Introduction

Diffusion-weighted magnetic resonance imaging (DWI) allows the early diagnosis of ischemic brain injury, which may be undetectable in computer tomography as well as in T2-weighted MRI [1]. The calculated "apparent diffusion coefficient" (ADC) reflects the mobility of water in tissues. Perfusion-weighted imaging (PWI) characterizes the perfusion state of brain tissues. However, prolonged mean transit times (MTT), pathologic relative cerebral blood volume (rCBV) etc. do not necessarily match with pathologic regions in DWI. Mismatching parts are thought to reflect brain tissues that can be saved by appropriate treatment [2]. The difficult task of segmenting healthy and different pathologic tissues was solved by combining DWI, PWI, and standard clinical imaging. Tissues were segmented according to their features represented by multidimensional histograms. Localization, extension, and structure of ischemic lesions were determined and their mean parameter values and standard deviations were stored in a tissue data base.

2 Materials and Methods

All examinations were conducted on a 1,5-Tesla magnetic resonance imaging system (Magnetom Vision, Siemens). Ten patients with cerebral ischemia were examined. All patients underwent standard T1- and T2-weighted (T1w, T2w) imaging as well as DWI and PWI within the first week after stroke onset. Segmentation of ischemic regions and unaffected parenchyma was performed by a radiologist.

2.1 Imageacquisition (DWI and PWI)

Single-shot spin echo EPI (echo planar imaging) with additional diffusion-weighting gradients was used for DWI. Pulse parameters were TE:112 ms, matrix size:128*96, 6 mm slice thickness, 20 slices were acquired. Four images with increasing diffusion weighting (b-factor 0, 511, 736, 1001 s/mm^2) were acquired for each slice. The ADC was calculated by linear-fitting the logarithm of the signal intensity versus increasing b-factors [3]. PWI was also performed with single-shot spin echo EPI. 60 measurements were acquired in 60 seconds (TE:65 ms, matrix:128*64, 6 mm slice thickness, 5 slices). Ten seconds after measurement begin 20 ml GaDTPA were administered.

All images were zero-filled to be displayed as 256*256 matrices. To minimize errors due to patient movements during the acquisition, all data sets were motion-corrected by image registration [4] before image postprocessing.

A gamma-variate function with an additional linear function was fitted to the signal change due to bolus transition using the Marquardt-Levenberg algorithm [5]. The fitted parameters led to the calculation of maps of MTT, rCBV and rCBF. The rCBV and MTT were calculated from the concentration-time curve, which could be obtained from the signal curve by the relation:

$$c(t) = \frac{1}{k}\frac{1}{TE}\ln\left(\frac{s_0}{s(t)}\right) \tag{1}$$

where k is a tissue- and pulse-sequence-specific constant, TE is the time-to-echo (65 ms), s(t) is the time-dependent signal intensity, and s_0 is the mean signal intensity prior to contrast agent administration. The rCBV is the first moment of the concentration-time course [6, 7]:

$$rCBV = K\int_0^\infty c(t)dt \tag{2}$$

where K is a proportionality factor that depends on the blood-tracer concentration and can not be determined from MRI data alone. The MTT is defined as the ratio of the first and zeroth moment of the concentration-time curve [6,7]:

$$MTT = \int_0^\infty t \cdot c(t)dt \Big/ \int_0^\infty c(t)dt \tag{3}$$

Some authors claim that this can only be seen as an approximation for the MTT, and that an appropriate physiological model for tissue blood flow is needed for an accurate approach [8,9]. To date, such a model is not available and therefore the first moment was used as an approximation for the MTT.

2.2 Segmentation

Multidimensional histograms were constructed by combining 1D histograms of selected parameter subsets. Histogram segmentation was performed using rectangular ROIs. In 2D histograms arbitrarily shaped ROIs could be additionally used. In a given histogram, voxels within the selected ranges of an ROI were color-encoded according to the parameter range and then superposed onto the original parameter images, allowing the visualization of both anatomical and physiological information. To determine the ADC values, the ADC map was combined with T2w images and DWI. For perfusion parameters T2w images or DWI were combined with rCBV, MTT, and rCBF maps. Mean values, standard deviations and extrema of the segmented ROIs were calculated and stored for further analysis. Using standard spread sheet analysis the changes of signals of the ischemic tissue relative to unaffected areas were calculated automatically for all stored parameters.

3 Results and Discussion

Method and representative results are illustrated in fig. 1 (patient 2). The ischemic regions are hyperintensely demarcated in the DWI (fig. 1a). ADC values (fig. 1b) are reduced within this region, however, their spatial distribution in the unaffected and in the ischemic regions are difficult to determine. Fig. 1c depicts the histogram of the DWI and the ADC map. ROI 1 corresponds to unaffected parenchyma, ROI 2 to the ischemia. Mean ADC of ROI 2 is reduced to 68% of normal (ROI 1), mean rCBV was reduced within ROI 2 (data not shown). A control examination (7 days later) showed increased ADC and T2-weighted values.

Table 1. Examination results: Mean signal changes of ischemic regions relative to unaffected areas for different imaging techniques and calculated maps.

Patient	days after stroke	signal value of lesion relative to unaffected parenchyma				
		T2w	*DWI*	*ADC*	*rCBV*	*MTT*
1	1	137%	254%	94%	192%	97%
2	7	118%	236%	68%	52%	114%
3	6	129%	186%	99%	62%	98%
4	4	121%	213%	80%	72%	110%
5	6	120%	175%	81%	74%	102%
6	7	176%	199%	93%	41%	148%
7	1	219%	265%	85%	53%	110%
8	7	179%	218%	114%	58%	130%
9	3	162%	263%	51%	115%	104%
10	6	178%	252%	84%	95%	110%

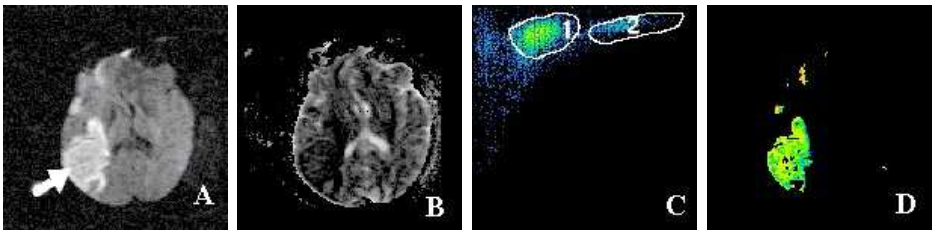

Fig. 1. Diffusion-weighted image (A). The ischemic regions are hyperintensely demarcated (arrow). The ADC map (B) shows a decrease of the ADC in the ischemic region. Histogram of DWI and ADC map (C) with regions of interest (ROI). Region 1 corresponds to unaffected gray and white matter and region 2 corresponds to the ischemic tissue. ADC values are ordered ascending in negative y-axis. Color-encoded overlay image (D) of ROI 2 depicts the ADC values of the ischemic regions.

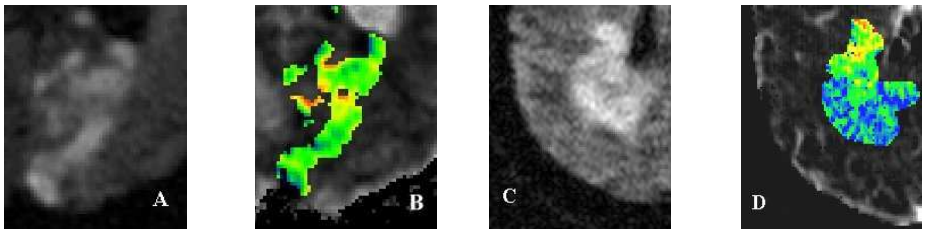

Fig 2. Spatial parameter distribution in ischemic lesions. A,B: The lesion is demarcated as a hyperintense region in the DWI (A; b-factor 1001 s/mm^2). The corresponding overlay of the histogram-based segmented ADC values (B) shows their spatial distribution within the scattered ischemic tissues. C,D: Perfusion parameters of a heterogeneously perfused lesion. The DWI (C) shows the hyperintense ischemic region, the corresponding overlay in the rCBF-map exhibits areas with high rCBF (green/yellow) as well as areas with decreased rCBF (blue).

The results of the examination are summarized in table 1. Eight patients showed prolonged MTT (see table 1) and reduced rCBV values within the lesion. Two patients showed increased mean rCBV (115 % and 192 %) within the whole lesion. Four patients allowed a differentiation of infarct regions with partially elevated rCBV and rCBF values (Fig 2c-d). However, for some ischemic regions a slow signal rise was observed in the late phase of the bolus passage. To fit this signal rise an additional linear function was required since a pure gamma-variate did not approximate the signal curve sufficiently. T2 was increased for all lesions, ADC values were reduced for all but one patient who exhibited slightly elevated values.

For all patients the combination of different information (T2, DWI, ADC, rCBV) allowed a clear separation of the lesions (Fig 2a-b). This is the prerequisite for the detection of even small relative ADC changes that may invert the sign during the first few 2 weeks. Quantitative ADC maps from patients with stroke are in good agreement with data found in the literature [1]. Since low ADC values with or without elevated T2 indicate acute ischemia whereas high ADC values and high T2 values are typical for old lesions [10], the above method enables an age estimation of different lesions and their perfusion state. This should provide a more accurate description on the time course of human infarcts.

4 Conclusion

Combining DWI, PWI, and standard imaging using a histogram-based data analysis overcomes problems of strongly fluctuating parameters such as ADC values. This led to good results in the determination and characterization of healthy and pathologic tissues by different parameter combinations. The feature-based analysis allowed a fast segmentation even of heterogeneous, scattered or small lesions that were otherwise difficult to characterize. Future examinations will investigate the details of different parameter characteristics, and the time courses of the ADC values and perfusion parameters for irreversibly and reversibly affected tissue.

5 References

1. Moseley ME, Cohen Y, Mintorovitch J, Chileuitt L, Shimizu H, Kucharczyk J, Wendland MF, Weinstein PR: Early detection of regional cerebral ischemia in cats: comparsion of diffusion- and T2-weightd MRI and spectroscopy. Magn. Reson. Med,. 14: 330-336, 1990.
2. Hossmann KA, Hoehn-Berlage M: Diffusion and PerfusionMR Imaging of Cerebral Ischemia. Cerebrovascular and Brain Metabolism Reviews, 7: 187-217, 1995.
3. Bernarding J, Braun J, et al.: Follow-up study of ischemic human cerebral tissue using com-bined diffusion-weighted imaging and relaxometry. Proc 7th Scient Meet ISMRM, Philadelphia: 211, 1999.
4. Woods RP, Grafton ST, Holmes CJ, Cherry SR, Mazziotta JC: Automated image registration: I. General methods and intrasubject, intramodality validation. Journal of Assisted Tomography, 22: 141-154, 1998.
5. Press WH, Teukolsky SA, Vetterling WT, Flannery BP: Numerical Recipes in C, 2nd Edition, Camebridge University Press, 1992.
6. Belliveau JW, Rosen BR, Kantor HL, Rzedzian RR, Kennedy DN, McKinstry RC, Vevea JM, Cohen MS, Pykett IL, Brady TJ: Functional crebral imaging by suceptibility-contrast NMR. Magn. Res. Med., 14: 538-546, 1990.
7. Norris DG, Hoehn-Berlage M, Wittlich F, Back T, Leibfritz D: Dynamic imaging with T2* contrast using U-FLARE, Magn. Res. Imag., 11: 921-924, 1993.
8. Hamberg LM, Macfarlane R, Tasdemiroglu E, Boccalini P, Hunter GJ, Belliveau JW, Moskowitz MA, Rosen BR: Measurement of cerebrovascular changes in cats after transient ischemia using dynamic magnetic resonance imaging,. Stroke, 25: 444-451, 1993.
9. Weisskoff Rm, Chesler D,Boxerman JL, Rosen BR: Pitfalls in MR measurement of tissue blood flow with intravascular tracers: which mean transit time? Magn. Res. Med., 29: 553-559, 1993.
10. Warach S, Gaa J, Siewert B, Wielopolski P, Edelman RR: Acute Human Stroke Studied by Whole Brain Echo Planar Diffusion-weighted Magnetic Resonance Imaging. Ann Neurol, 37: 231-241, 1995.